Control of UUVs Based upon Mathematical Models Obtained from Self-Oscillations Experiments

Nikola Miskovic * **Zoran Vukic** * **Edin Omerdic** **

* *University of Zagreb, Faculty of Electrical Engineering and Computing, Unska 3, Zagreb, Croatia (e-mail: nikola.miskovic, zoran.vukic@fer.hr).*
** *Mobile & Marine Robotics Research Centre, University of Limerick, Limerick, Ireland, (e-mail: edin.omerdic@ul.ie)*

Abstract: The paper describes the use of self-oscillation identification method for controller design for underwater vehicles. Using the proposed algorithm both linear and nonlinear models can be obtained. In addition to that, the algorithm enables identification of the bias term that appears due to currents (in yaw models) and difference between weigh and buoyancy (in heave models). A detailed stability analysis has been performed for the proposed controller which is either linear or nonlinear based on the assumption on the process model. Simulation results are presented for two underwater vehicles.

Keywords: underwater vehicle, parameter identification, self-oscillations, nonlinear models, nonlinear control

1. INTRODUCTION

The complete control architecture of vehicles can be divided in three major levels: low, mid and high, Miskovic et al. (2006). While mid and high levels are in charge for trajectory planning and mission control, respectively, low level controls all controllable degrees of freedom of a vehicle. In order to achieve satisfactory performance at higher levels, low level control should be designed properly. In most cases, low level control architecture includes yaw, surge and depth control. Many algorithms have been developed for control of these degrees of freedom, starting from linear PID controllers all the way to intelligent controllers, Fossen (1994), Caccia and Veruggio (2000). Classical methods used for identification usually require a great number of experiments in order to obtain a satisfactory model, Ljung (1999), Fossen (1994), Caccia et al. (2000), Caccia et al. (2006), Miskovic et al. (2007a), Ridao et al. (2004), Stipanov et al. (2007). The advantage of these methods is that the more data is available, the more precise model can be obtained. The greatest disadvantage is that they are time-consuming and disturbances have significant influence on the results. The most popular identification method for marine vehicles is the "zig-zag" manoeuver, López et al. (2004). The advantage of this method is that the disturbances are partially compensated due to the closed-loop and the experiment itself is not time-consuming. However, this method gives only linear models of marine vehicles.

In Section II the self-oscillation identification method is briefly described. The full description can be found in Miskovic et al. (2007c) and Miskovic et al. (2007b). The method is also augmented for systems with bias signals. In Section III I-PD controller design for heading and depth control is presented. The controller is of I-PD type and is designed in such a way that system nonlinearities are compensated if they exist. The greatest advantage is that this controller gives smooth control action, Vukic and Kuljaca (2005). In addition to that, a proof of stability is given with reflection to structural stability of the closed loop system. Section IV gives simulation examples for control of heading and depth of the FALCON ROV and heading of VideoRay Automarine AUV. The paper is concluded with Section V.

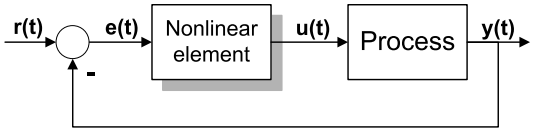

Fig. 1. Closed-loop scheme for inducing self-oscillations.

2. IDENTIFICATION BY USE OF SELF-OSCILLATIONS

The self-oscillations identification method can be used to determine parameters of linear and nonlinear models under the assumption that the model structure is known. The method is based upon forcing the system into self-oscillations. The experiment for that is done in closed-loop which consists of the process itself and a nonlinear element, as shown in Fig. 1.

The nonlinear element should be chosen in such a way that oscillations can be obtained. The most common nonlinearity used in practice is a relay with hysteresis since it can cause self-oscillations in every system whose Nyquist characteristic passes through the III quadrant, Vukic et al. (2003) and Netushil (1978).

While describing marine vehicle dynamics, usually two models are used: the linear one, (1) which has a constant drag, and the nonlinear one, (2) whose drag is linear, Fossen (1994), Caccia et al. (2000). In both models, variable x is usually heading, ψ, depth, z, or any other degree of freedom which is to be controlled. Parameter τ is the excitation force (e.g. surge force, yaw moment). Parameter δ can either be external disturbance (in the case of identifying yaw model) or a vehicle physical parameter such as difference between weigh and buoyancy (in the case of identifying heave model).

$$\alpha\ddot{x}(t) + k_x\dot{x}(t) + \delta = \tau(t) \tag{1}$$

$$\alpha\ddot{x}(t) + k_{xx}|\dot{x}(t)|\dot{x}(t) + \delta = \tau(t) \tag{2}$$

2.1 Identification of α, k_x and k_{xx}

For now, let us assume that $\delta = 0$. If a system can be described with (1) or (2) the unknown parameter α can be identified using (3). If the system can be described with (1) than parameter k_x can be identified using (4). On the other hand, (5) is used if a system can be described with (2) and k_{xx} should be identified, see Miskovic et al. (2007c) and Miskovic et al. (2007b).

$$\alpha = \frac{P_N(X_m)}{\omega^2} \tag{3}$$

$$k_x = -\frac{Q_N(X_m)}{\omega} \tag{4}$$

$$k_{xx} = -\frac{3\pi}{8}\frac{Q_N(X_m)}{X_m\omega^2} \tag{5}$$

In (3), (4) and (5) ω is the frequency and X_m magnitude of self-oscillations, $P_N(X_m)$ and $Q_N(X_m)$ are real and imaginary parts of the describing function of the nonlinear element respectively. For the relay with hysteresis, $P(X_m) = \frac{4C}{\pi X_m}\sqrt{1-\left(\frac{x_a}{X_m}\right)^2}$ and $Q(X_m) = -\frac{4C}{\pi X_m^2}x_a$ where C is relay output, and x_a relay width, Vukic et al. (2003).

The main assumptions that are posed on given equations are that the oscillations are symmetric and that higher harmonics are negligible in comparison to the first harmonic. For more details on derivation of the given equations, the reader is referred to Miskovic et al. (2007c), Miskovic et al. (2007b) and Vukic et al. (2003).

2.2 Identification of δ

If a general process of n-th order, includes a constant term δ, i.e. it can be presented as $f\left(\frac{d^n x(t)}{dt^n}, \cdots, x(t), \delta\right) = \tau(t)$, self-oscillations will not be symmetric. If T_H represents the time when relay output is in "high" position, and T_L represents the time when relay output is in "low" position, T_H will differ from T_L as shown in Fig. 2. This means that equations (3), (4), and (5) are not valid. However, based on times T_H and T_L the bias term can be determined, using (6) and thus compensated for within the controller.

$$\frac{C+\delta}{-(-C+\delta)} = \frac{T_H}{T_L} \Rightarrow \delta = C\frac{T_H - T_L}{T_H + T_L} \tag{6}$$

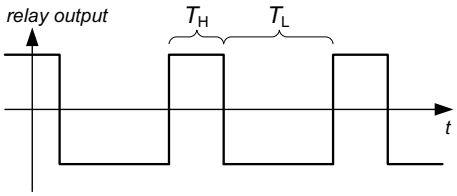

Fig. 2. Asymmetric output from the relay with hysteresis

3. CONTROLLER DESIGN

In this section we will present a controller which is designed based on a model function. Using the proposed controller, even a nonlinear process will give desired response. This will be achieved by compensating the nonlinearity which arises in the system itself. Under the assumption that the process in general can be written using

$$\alpha\ddot{x}(t) + \varepsilon\dot{x}(t) = \tau(t), \tag{7}$$

where

$$\varepsilon = \begin{cases} k_x & \text{for linear model} \\ k_{xx}|\dot{x}| & \text{for nonlinear model} \end{cases},$$

the I-PD controller algorithm has the equation given with (8), Vukic and Kuljaca (2005).

$$\tau(t) = K_I\int_0^t [x_{ref}(t) - x(t)]\,dt - K_P x(t) - K_D\dot{x}(t) \tag{8}$$

Using the proposed control algorithm, the closed loop equation is

$$\frac{x}{x_{ref}} = \frac{1}{\frac{\alpha}{K_I}s^3 + \frac{\varepsilon+K_D}{K_I}s^2 + \frac{K_P}{K_I}s + 1}. \tag{9}$$

The controller parameters are set so that the closed-loop transfer function is equal to the model function $G_m(s) = \frac{1}{a_3s^3+a_2s^2+a_1s+1}$ which is stable. In that case, the controller parameters will be as follows:

$$K_I = \frac{\alpha}{a_3}, K_P = \frac{a_1}{a_3}\alpha, K_D = \frac{a_2}{a_3}\alpha - \varepsilon. \tag{10}$$

This controller can be used for controlling yaw and heave motion (which will be demonstrated in this paper) as well as other degrees of freedom.

3.1 Heading Control

Yaw motion of an underwater vehicle is usually described by using two simple models:

- linear, (1), where $x = \psi$, $\tau = \tau_N$, $\alpha = I_r$, $\varepsilon = k_r$ and $\delta = 0$ give model $I_r\ddot{\psi} + k_r\dot{\psi} = \tau_N$. If unknown parameters are estimated using the self-oscillation method so that $\tilde{I}_r$ and $\tilde{k}_r$ are obtained using (3) and (4), the following set of controller parameters is obtained:

$$\tilde{K}_I = \frac{\tilde{I}_r}{a_3}, \tilde{K}_P = \frac{a_1}{a_3}\tilde{I}_r, \tilde{K}_D = \frac{a_2}{a_3}\tilde{I}_r - \tilde{k}_r \tag{11}$$

- nonlinear, (2), where $x = \psi$, $\tau = \tau_N$, $\alpha = I_r$, $\varepsilon = \varepsilon\left(\dot{\psi}\right) = k_{rr}\left|\dot{\psi}(t)\right|$ and $\delta = 0$ give model

$I_r\ddot{\psi} + k_{rr}\left|\dot{\psi}\right|\dot{\psi} = \tau_N$. It should be noticed that in this case parameter ε varies in time and $\tilde{k}_{rr}$ is obtained using (5), giving the time-variant controller parameters of a form:

$$\tilde{K}_I = \frac{\tilde{I}_r}{a_3}, \tilde{K}_P = \frac{a_1}{a_3}\tilde{I}_r, \tilde{K}_D = \frac{a_2}{a_3}\tilde{I}_r - \tilde{k}_{rr}\left|\dot{\psi}(t)\right|. \quad (12)$$

3.2 Depth Control

Just as in the case of yaw motion control, heave motion is usually described using the linear, (1), or the nonlinear model, (2). However, in this case there will exist a bias term δ which represents the difference between the weight and buoyancy of the vehicle. This term can be compensated by adding an estimated bias $\tilde{\delta}$ to the controller action (8). Now, the two models can be written in the following form:

- linear, (1), where $x = z$, $\tau = \tau_Z$, $\alpha = m_z$ and $\varepsilon = k_w$ give model $m_z\ddot{z} + k_w\dot{z} + \delta = \tau_Z$. If unknown parameters are estimated using the self-oscillation method so that $\tilde{m}_z$, $\tilde{k}_w$ and $\tilde{\delta}$ are obtained using (3), (4), and (6), the following set of controller parameters is obtained:
$$\tilde{K}_I = \frac{\tilde{m}_z}{a_3}, \tilde{K}_P = \frac{a_1}{a_3}\tilde{m}_z, \tilde{K}_D = \frac{a_2}{a_3}\tilde{m}_z - \tilde{k}_w \quad (13)$$
- nonlinear, (2), where $x = z$, $\tau = \tau_Z$, $\alpha = m_z$ and $\varepsilon = \varepsilon(\dot{z}) = k_{ww}|\dot{z}(t)|$ give model $m_z\ddot{z} + k_{ww}|\dot{z}(t)|\dot{z} + \delta = \tau_Z$. Again, parameter ε varies in time and is obtained using (5), giving the time-variant controller parameters of a form:
$$\tilde{K}_I = \frac{\tilde{m}_z}{a_3}, \tilde{K}_P = \frac{a_1}{a_3}\tilde{m}_z, \tilde{K}_D = \frac{a_2}{a_3}\tilde{m}_z - \tilde{k}_{ww}|\dot{z}(t)| \quad (14)$$

For both yaw and heave control cases, the controller can be presented with a general structure shown in Fig. 3, which will be explained after the following subsection.

3.3 Stability Analysis

It is shown in Miskovic et al. (2007b) that the self-oscillation identification method has a certain error. The stability of the closed-loop system could be compromised if the identified parameters are not identical to real process parameters (robust stability) or if the process has a structure different than the one that is assumed (structural stability). Because of the two reasons, we will observe stability of the closed-loop system with regard to the following propositions.

Proposition 1. Identified parameters $\tilde{\alpha}$ and $\tilde{\varepsilon}$ may differ from real parameters α and ε.

Proposition 2. The process may not have the structure which can be described with (1) or (2), but with a more general, affine equation (15).

$$\alpha\ddot{x}(t) + k_x\dot{x}(t) + k_{xx}|\dot{x}(t)|\dot{x}(t) = \tau(t) \quad (15)$$

Proposition 3. The controller is always designed under the assumption that the process structure can be described with (1) or (2).

Because of Proposition 1, the controller parameters are written in the following form:

$$\tilde{K}_I = \frac{\tilde{\alpha}}{a_3}, \tilde{K}_P = \frac{a_1}{a_3}\tilde{\alpha}, \tilde{K}_D = \frac{a_2}{a_3}\tilde{\alpha} - \tilde{\varepsilon} \quad (16)$$

where

$$\tilde{\varepsilon} = \begin{cases} \tilde{k}_x & \text{for linear controller} \\ \tilde{k}_{xx}|\dot{x}| & \text{for nonlinear controller} \end{cases}.$$

In this case, the closed loop can be described with (17).

$$\frac{x}{x_{ref}} = \frac{1}{\frac{\alpha}{\tilde{\alpha}}a_3 s^3 + \left[a_2 + a_3\frac{\varepsilon-\tilde{\varepsilon}}{\alpha}\right]s^2 + a_1 s + 1} \quad (17)$$

It should be noticed that in the case of exact parameter identification for values $\tilde{\alpha} = \alpha$ and $\tilde{\varepsilon} = \varepsilon$ the model function itself is obtained. From the characteristic equation of the system, stability of the closed loop can be determined by using the Jury criterion, Vukic and Kuljaca (2005). Conditions $\frac{\alpha}{\tilde{\alpha}}a_3 > 0$ and $a_1 > 0$ are always satisfied. Remaining condition $a_2 + a_3\frac{\varepsilon-\tilde{\varepsilon}}{\tilde{\alpha}} > 0$ can be written in the following form:

$$\tilde{\varepsilon} - \varepsilon < \frac{a_2}{a_3}\tilde{\alpha}. \quad (18)$$

Another condition from Jury criterion which must be fulfilled is

$$\tilde{\varepsilon} - \varepsilon < \frac{a_2}{a_3}\tilde{\alpha} - \frac{1}{a_1}\alpha. \quad (19)$$

By observing the sign of the right-hand side of (19), we get

$$\frac{\tilde{\alpha}}{\alpha} \overset{?}{>} \frac{a_3}{a_2 a_1}. \quad (20)$$

If the model function is a 3rd order Butterworth filter than $\frac{\tilde{\alpha}}{\alpha} > 0.25$ and for 3rd order Bessel filter $\frac{\tilde{\alpha}}{\alpha} > 0.1667$. This implies that (20) is always satisfied (see parameter error analysis in Miskovic et al. (2007b)). This means that the right-hand side of (19) is always greater than 0. The conclusion is that condition (19) is stricter than condition (18) and therefore it will be used for determining stability. Further on, from (19), if $\tilde{\varepsilon} - \varepsilon < 0$ the system is always stable. If $\tilde{\varepsilon} - \varepsilon > 0$ a constraint on the system stability is obtained. For further calculus, ratios between the identified parameters and real parameters are defined:

$$\begin{aligned} \frac{\tilde{\alpha} - \alpha}{\alpha} &= p_\alpha \Rightarrow \alpha = \frac{\tilde{\alpha}}{p_\alpha + 1}, p_\alpha \in (-1, 1) \\ \frac{\tilde{\varepsilon} - \varepsilon}{\varepsilon} &= p_\varepsilon \Rightarrow \varepsilon = \frac{\tilde{\varepsilon}}{p_\varepsilon + 1}, p_\varepsilon \in (-1, 1) \end{aligned}.$$

It was mentioned before that for $p_\varepsilon < 0$ the system is always stable, therefore the assumption for further analysis is that $p_\varepsilon > 0$. From Proposition 2 and Proposition 3 follows that there are four different cases: when linear controller with parameters (11) is used with linear model (1) and affine model (15), and when nonlinear controller with parameters (12) is used with nonlinear model (2) and affine model (15).

Linear model & linear controller. For this case the model has $\varepsilon = k_x$ and the controller $\tilde{\varepsilon} = \tilde{k}_x$. From (19) follows that (21) has to be fulfilled in order to have stable closed-loop system.

$$1 < \frac{\frac{a_2}{a_3}\tilde{\alpha} - \frac{1}{a_1}\alpha}{\tilde{k}_x - k_x} \quad (21)$$

Using the ratios, (22) is obtained.

$$\frac{\tilde{k}_x}{\tilde{\alpha}} \frac{p_{kx}}{p_{kx}+1} - \frac{a_2}{a_3} < -\frac{1}{a_1} \frac{1}{p_\alpha + 1} \tag{22}$$

This inequality gives an elegant method of determining stability of the closed system after the system parameters have been identified. With estimated errors of identification, bounds can be set on the model function in order to ensure stability. If it is assumed that the identification experiment is carried out in such a way that the absolute error in determining k_x is definitely smaller than 20%, we write $|p_{kx}| < 0.2$. If this is the case, than parameter α has an absolute error lower than 10% (see parameter identification errors in Miskovic et al. (2007b)), i.e. $|p_\alpha| < 0.1$. The worst case for stability condition (22) is when $p_{kx} = 0.2$ and $p_\alpha = -0.1$, which gives (23).

$$\frac{\tilde{k}_x}{\tilde{\alpha}} < \frac{2}{3} \frac{9a_1a_2 - 10a_3}{a_1a_3} \tag{23}$$

Affine model & linear controller. For this case the model has $\varepsilon = k_{xx}|\dot{x}| + k_x$ and the controller $\tilde{\varepsilon} = \tilde{k}_x$. From (19) follows that (24) has to be fulfilled in order to have stable closed-loop system.

$$\tilde{k}_x - k_x < \frac{a_2}{a_3}\tilde{\alpha} - \frac{1}{a_1}\alpha + k_{xx}|\dot{x}| \tag{24}$$

By comparing (22) and (24) we see that condition (22) is stricter - if the stability is ensured for the previous case, this case will also be stable. However, while designing the controller, one should bear in mind that the differences between the identified and real parameters might be greater.

Nonlinear model & nonlinear controller. For this case the model has $\varepsilon = k_{xx}|\dot{x}|$ and the controller $\tilde{\varepsilon} = \tilde{k}_{xx}|\dot{x}|$. From (19) follows that (25) has to be fulfilled in order to have stable closed-loop system.

$$|\dot{x}| < \frac{\frac{a_2}{a_3}\tilde{\alpha} - \frac{1}{a_1}\alpha}{\tilde{k}_{xx} - k_{xx}} \tag{25}$$

Using the ratios, (26) is obtained.

$$|\dot{x}| < \frac{\tilde{\alpha}}{\tilde{k}_{xx}} \frac{p_{kxx}+1}{p_{kxx}} \left(\frac{a_2}{a_3} - \frac{1}{a_1} \frac{1}{p_\alpha + 1} \right) \tag{26}$$

This inequality does not provide stability condition immediately after the parameters have been identified, but it can be used to set a limit to the derivative control action of the controller. This limitation in the controller will ensure the stability of the system. If the same identification errors as described before are assumed, i.e. $p_{kx} = 0.2$ and $p_\alpha = -0.1$, the worst case scenario gives limitation (27).

$$|\dot{x}| < \frac{2}{3} \frac{\tilde{\alpha}}{\tilde{k}_{xx}} \frac{9a_1a_2 - 10a_3}{a_1a_3} \tag{27}$$

Affine model & nonlinear controller. For this case the model has $\varepsilon = k_{xx}|\dot{x}| + k_x$ and the controller $\tilde{\varepsilon} = \tilde{k}_{xx}|\dot{x}|$. From (19) follows that (28) has to be fulfilled in order to have stable closed-loop system.

$$|\dot{x}| \left(\tilde{k}_{xx} - k_{xx} \right) < \frac{a_2}{a_3}\tilde{\alpha} - \frac{1}{a_1}\alpha + k_x \tag{28}$$

By comparing (26) and (28) we see that condition (26) is stricter, which means that false assumption on the process' structure will not cause instability. However, in this case one should be careful while limiting $\dot{x}$ because the estimation errors may be larger than in the previous case.

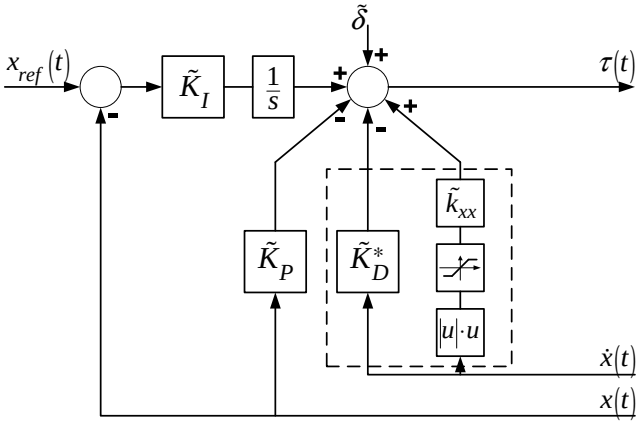

Fig. 3. The I-PD controller structure

After having defined the stability bounds for the closed-loop system, we can describe in detail the general controller given in Fig. 3. Parameter $\tilde{K}_D^* = \frac{a_2}{a_3}\tilde{\alpha}$ is the part of $\tilde{K}_D$ that does not change whether the controller is linear, as in (11), or nonlinear, as in (12). Parameter $\tilde{k}_{xx}$ equals 0 if the controller is linear. The limiter which is in the derivation channel is here to ensure stability of the closed loop. If the process is linear, and can be described with (1), the limiter does not have any function since this channel does not exist and stability is determined immediately after calculating the controller parameters. If the process is nonlinear, and can be described with (2), the lower limit to the saturation block is 0, while the upper limit is given with (26).

4. SIMULATION RESULTS

For all the simulation examples, two experiments were performed. The first one which is used for identification purposes, i.e. the ratio between the input to the relay with hysteresis and hysteresis width is as close to 1.5 as possible, see Miskovic et al. (2007c), and the second experiment which is used for determining the model. If the second experiment, which is less accurate than the first one, shows that the identified parameter k_x has changed its value less than the identified parameter k_{xx}, than the model that best describes the system dynamics is linear. If parameter k_x changes its value more than parameter k_{xx} than a nonlinear model is presumed. In both experiments the value of α should be similar, which shows that both experiments are reliable. If the system model is known from before than the second experiment need not be conducted.

4.1 FALCON ROV

The real yaw model parameters of the FALCON vehicle are shown in Table 1. The results of the two self-oscillation experiments that were performed for yaw degree of freedom are shown in Table 2.

Table 1. FALCON ROV yaw model parameters

I_r	k_r	k_{rr}
80	300	10

Table 2. Self-oscillation data for FALCON ROV yaw model identification

	$X_m[°]$	$\omega[s^{-1}]$	$\tilde{I}_r$	$\tilde{k}_r$	$\tilde{k}_{rr}$
$x_a = 10°$ $C = 300$	14	3.722	78.97	298.48	385.66
$x_a = 20°$ $C = 300$	24.4	2.547	79.29	288.3 (↓ 3.4%)	312.97 (↓ 18.9%)

The first experiment gives ratio $\frac{X_m}{x_a} = 1.4$ and the second $\frac{X_m}{x_a} = 1.22$. Since the first experiment has the ratio closer to 1.5, it will be used for identification. The second one will be used for model determination. Since the value of $\tilde{k}_r$ has changed less in the two experiments than the value of $\tilde{k}_{rr}$, linear yaw model of the vehicle will be presumed. However, it should be noticed that the real vehicle dynamics also include a k_{rr} term. Based on these identification results, a linear I-PD controller with parameters according to (11) can be designed so that a 3rd order Bessel filter with characteristic frequency $\omega_0 = 1.5\frac{rad}{s}$ behavior is achieved. This model function is chosen so that the vehicle could perform a 90° turn without the thrusters saturating. Using the stability condition (23) we get $3.78 < 17.84$ which proves the stability of the designed closed loop. The simulation results are shown in Fig. 4.

The real heave model parameters of the FALCON vehicle are shown in Table 3. Due to the difference between the weigh and buoyancy of the vehicle, the oscillations that are obtained are not symmetric, as it is shown in Fig. 5 As it was explained in Section I, using the periods of "low" and "high" controller outputs, the bias term can be determined by using (6). However, it should be mentioned that responses in Fig. 5 are not in concordance to the real FALCON ROV heave model, but have been obtained for demonstration purposes in such a way that the difference between weigh and buoyancy was enlarged in order to emphasize the asymmetric response. The results of the two self-oscillation experiments that were performed for yaw are shown in Table 4.

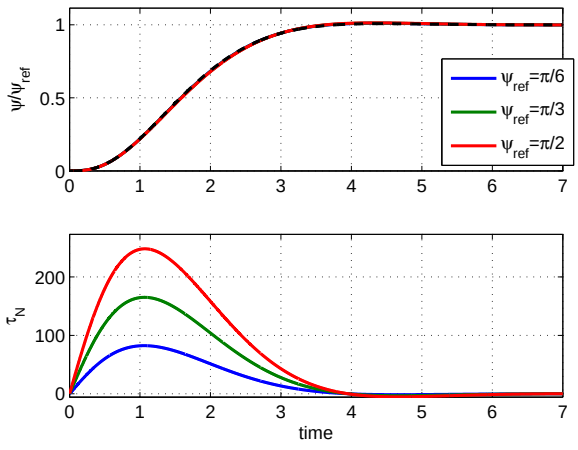

Fig. 4. FALCON ROV heading response

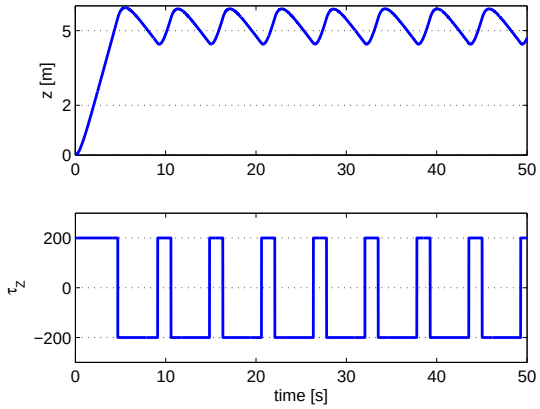

Fig. 5. FALCON ROV self-oscillations experiment for determining heave model

The first experiment gives ratio $\frac{X_m}{x_a} = 1.328$ and the second $\frac{X_m}{x_a} = 1.188$. As in the yaw model identification case, first experiment will be used for identification and linear model will be assumed. Again, the real vehicle dynamics include a k_{ww} term also. Based on these identification results, a linear I-PD controller with parameters according to (13) can be designed so that a 3rd order Bessel filter with characteristic frequency $\omega_0 = 0.8\frac{rad}{s}$ behavior is achieved. This model function is chosen so that the vehicle could perform a $3m$ dive without the thrusters saturating. Using the stability condition (23) we get $1.61 < 9.5153$ which proves the stability of the designed closed loop. The simulation results are shown in Fig. 6.

4.2 VideoRay Automarine AUV

The real yaw model parameters of the VideoRay Automarine vehicle were obtained in Stipanov et al. (2007) and are shown in Table 5. The results of the two self-oscillation experiments that were performed for yaw degree of freedom are shown in Table 6. In this case both experiments give approximately the same $\frac{X_m}{x_a}$ ratios. This is usually one of the indicators that the system has dominantly linear drag. By comparison of the identified parameters from the two experiments, we can conclude that since the value of $\tilde{k}_{rr}$ has changed less in the two experiments than the value of $\tilde{k}_r$, nonlinear yaw model (2) (linear drag) of the vehicle will be presumed. Based on these identification results, a nonlinear I-PD controller with parameters according to (12) can be designed so that a 3rd order Bessel filter with characteristic frequency $\omega_0 = 1.5\frac{rad}{s}$ behavior is

Table 3. FALCON ROV heave model parameters

m_w	k_w	k_{ww}	δ
130	200	20	10

Table 4. Self-oscillation data for FALCON ROV heave model identification

	$X_m[°]$	$\omega[s^{-1}]$	$\tilde{m}_w$	$\tilde{k}_w$	$\tilde{k}_{ww}$
$x_a = 0.5m$ $C = 200$	0.664	1.405	127.79	205.75	259.94
$x_a = 0.5m$ $C = 100$	0.594	0.935	132.28	192.86 (↓ 6.3%)	408.81 (↑ 57.3%)

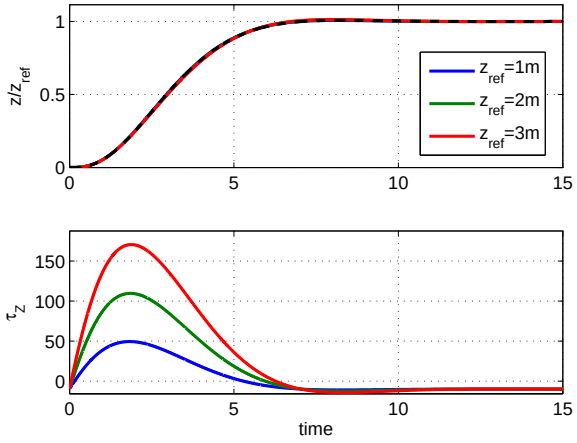

Fig. 6. FALCON ROV depth response

Table 5. VideoRay Automarine AUV yaw model parameters

I_r	k_r	k_{rr}
1.018	0	1.257

Table 6. Self-oscillation data for VideoRay Automarine AUV yaw model identification

	$X_m[°]$	$\omega[s^{-1}]$	$\tilde{I}_r$	$\tilde{k}_r$	$\tilde{k}_{rr}$
$x_a = 20°$ $C = 1$	35.12	1.32	0.98	0.896	1.305
$x_a = 20°$ $C = 0.8$	35.32	1.18	0.984	0.795 (↓ 11%)	1.292 (↓ 1%)

achieved. This model function is chosen so that the vehicle could perform a 90° turn without the thrusters saturating. Using the stability condition (27) we get that $|\dot{\psi}| < 13.4$ in order to have a stable closed loop. The simulation results are shown in Fig. 7 and in the third graph of the same figure it can be seen that $|\dot{\psi}|$ never passes the critical value, i.e. the limit in the controller in Fig. 3 is never reached.

5. CONCLUSION

The paper demonstrates how mathematical models obtained from self-oscillations experiments can be used to tune controllers for underwater vehicles. The proposed controller is of I-PD type and can compensate nonlinear behavior of the system. The controller is suitable for marine applications since the control signal is smooth. The stability analysis of the proposed control structure gives conditions under which the system is stable.

ACKNOWLEDGEMENTS

The work was carried out in the framework of the research project "RoboMarSec - Underwater robotics in sub-sea protection and maritime security" supported by the Ministry of Science, Education and Sport of the Republic of Croatia (Project No.036-0362975-2999).

REFERENCES

M. Caccia and G. Veruggio. Guidance and control of a reconfigurable unmanned underwater vehicle. *Control Engineering Practice*, 8(1):21–37, 2000.

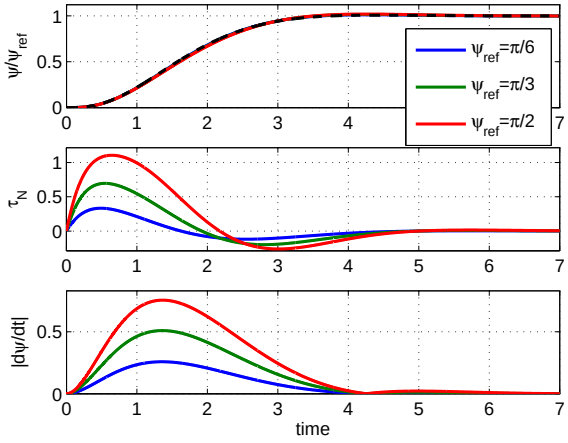

Fig. 7. VideoRay Automarine AUV heading response

M. Caccia, G. Indiveri, and G. Veruggio. Modelling and identification of open-frame variable configuration underwater vehicles. *IEEE Journal of Ocean Engineering*, 25(2):227–240, 2000.

M. Caccia, G. Bruzzone, and R. Bono. Modelling and identification of the Charlie2005 ASC. *Proc. of IEEE 14th Mediterranean Conference on Control and Automation*, 2006.

T.I. Fossen. *Guidance and Control of Ocean Vehicles*. John Wiley & Sons, 1994.

L. Ljung. *System Identification - Theory for the User*. Prentice Hall, 1999.

E. López, F.J. Velasco, E. Moyano, and T.M. Rueda. Full-scale manoeuvering trials simulation. *Journal of Maritime Research*, 1(3):37–50, 2004.

N. Miskovic, Z. Vukic, M. Barisic, and B. Tovornik. Autotuning autopilots for micro-ROVs. *Proc. of the 14th Mediterranean Conference on Control and Applications*, 2006.

N. Miskovic, Z. Vukic, and M. Barisic. Identification of coupled mathematical models for underwater vehicles. *Proc. of the OCEANS'07 Conference*, 2007a.

N. Miskovic, Z. Vukic, M. Barisic, and P.P. Soucacos. AUV identification by use of self-oscillations. *Proc. of the CAMS'07 Conference*, 2007b.

N. Miskovic, Z. Vukic, M. Barisic, and B. Tovornik. Transfer function identification by using self-oscillations. *Proc. of the 15th Mediterranean Conference on Control and Applications*, 2007c.

A. Netushil. *Theory of Automatic Control*. Mir Publishers, Moscow, 1978.

P. Ridao, A. Tiano, A. El-Fakdi, M. Carreras, and A. Zirilli. On the identification of non-linear models of unmanned underwater vehicles. *Control Engineering Practice*, 12:1483–1499, 2004.

M. Stipanov, N. Miskovic, Z. Vukic, and M. Barisic. ROV autonomization - yaw identification and Automarine module architecture. *Proc. of the CAMS'07 Conference*, 2007.

Z. Vukic and Lj. Kuljaca. *Automatic Control - Analysis of Linear Systems*. Kigen, Zagreb, 2005.

Z. Vukic, Lj. Kuljaca, D. Donlagic, and S. Tesnjak. *Nonlinear Control Systems*. Marcel Dekker, New York, 2003.